

Microvascular Changes in the Cystic Lesion of Branch Retinal Vein Occlusion Imaged by Swept-Source Optical Coherence Tomography Angiography

Satoko Araki^a Susumu Sakimoto^{a, b} Daiki Shiozaki^a Chihiro Ueda^a
Chikako Hara^a Yoko Fukushima^{a, b} Kaori Sayanagi^a Hirokazu Sakaguchi^c
Kohji Nishida^{a, b}

^aDepartment of Ophthalmology, Osaka University Graduate School of Medicine, Suita, Japan; ^bIntegrated Frontier Research for Medical Science Division, Institute for Open and Transdisciplinary Research Initiatives, Osaka University, Suita, Japan; ^cDepartment of Ophthalmology, Gifu University Graduate School of Medicine, Gifu, Japan

Keywords

Optical coherence tomography · Branch retinal vein occlusion · Vascular endothelial growth factor

Abstract

Introduction: This study aimed to describe the quantitative features of the microvasculature in the cystic lesions of branch retinal vein occlusion (BRVO). **Methods:** A total of 43 eyes with BRVO, treated with anti-vascular endothelial growth factor therapy, were analyzed. Using wide-field swept-source optical coherence tomography angiography (OCTA), en face OCT images were obtained by depth-integrated reflectivity of the retina, and vascular density (VD), vascular length (VL), vascular lacunarity, and fractal dimension (FD) were evaluated in a 12 × 12-mm area of retinal non-perfusion. **Results:** The mean area of affected lesions was 38.7 ± 19.8 mm², and cystic lesions were 8.5 ± 10.1 mm². VD, VL, and FD were significantly decreased in the cystic lesions compared to other affected lesions in the same eyes ($p = 0.0010$, $p = 0.0001$, and $p = 0.0003$, respectively) and in all eyes ($p = 0.0281$, $p = 0.0050$, and $p < 0.0001$, respectively). VD in cystic lesions within the vascular arcade (25 eyes) corre-

lated with best-corrected visual acuity on OCTA ($r = -0.433$, and $p = 0.0492$). **Conclusions:** Vascular structure in the cystic lesions was unpreserved compared to the other lesions in BRVO. These findings may help in understanding the pathophysiology of retinal edema in BRVO.

© 2022 The Author(s).
Published by S. Karger AG, Basel

Introduction

In branch retinal vein occlusion (BRVO), increased vascular permeability triggered by vascular endothelial growth factor (VEGF) leads to accumulation of intraretinal fluid in the affected region. The most common cause of decreased vision in BRVO is macular edema, and anti-VEGF therapy is the first line of treatment [1, 2]. The fact that symptoms such as retinal hemorrhage, retinal non-perfusion, and macular edema have been shown to resolve with anti-VEGF therapy has convinced ophthalmologists that VEGF has a pivotal role in the pathogenesis of BRVO [1, 3]. Retinal nonperfusion, which induces VEGF expression, is usually visualized by fluorescein an-

giography (FA) or optical coherence tomography angiography (OCTA).

OCTA can visualize retinal vasculature at a relatively high axial resolution without using dye injections [4, 5]. Motion contrast, induced by reflectivity changes between multiple OCT B-scans, detects the flow of blood cells in the retina [6, 7]. Previous reports have focused on limited areas, mainly 3×3 -mm macular scans [4, 8]. In contrast, high-speed, 1,050-nm central wavelength swept-source OCTA (SS-OCTA; PLEX[®] Elite 9000; Carl Zeiss Meditec, Jena, Germany) showed retinal vessels in relatively large scan areas ($12 \text{ mm} \times 12 \text{ mm}$). FA is evidently valuable for detecting both the location and degree of retinal nonperfusion; however, to elucidate detailed relationships between the configurations of retinal structure and perfusion status, specialized conjunctions with OCT and FA imaging are required [9, 10].

Previously, lesions of retinal nonperfusion were analyzed using en face OCT in conjunction with FA [9]. Depth-integrated en face OCT images showed a two-dimensional honeycomb-like structure in areas of retinal nonperfusion with retinal edema. Although retinal nonperfusion can be detected by OCTA, a detailed morphological analysis of the retinal cystic lesion using OCTA has not yet been reported. To our knowledge, the current study is the first to demonstrate the efficacy of wide-field SS-OCTA in visualizing the microvasculature in the cystic lesions in eyes with BRVO. Additionally, we analyzed the microvascular structure to validate its significance in the pathogenesis of BRVO.

Methods

We retrospectively reviewed 66 consecutive patients with BRVO between April and August 2018 at a single academic institution. The institutional review board of Osaka University Hospital approved the study protocol (approval number: 09260), and informed consent was obtained from the patients after an explanation of the nature and possible consequences of the study. The inclusion criteria were (1) eyes with BRVO treated with a pro re nata anti-VEGF therapy, (2) wide-field OCTA images of sufficient quality obtained using wide-field SS-OCTA scans (PLEX[®] Elite 9000) of 12×12 -mm regions of retinal nonperfusion, and (3) a symptom duration less than 60 months [11]. To obtain images of sufficient quality, independent of retinal hemorrhage, we excluded patients with symptom duration less than 3 months. Eyes that previously underwent vitrectomy or laser photocoagulation within the vascular arcade (25 eyes), eyes that received intravitreal injection of an anti-VEGF agent 3 months before SS-OCTA was performed, and eyes with coexisting ocular diseases, such as epiretinal membrane, glaucoma, or proliferative diabetic retinopathy (DR), were also excluded. BRVO was diagnosed based on a comprehensive ophthalmologic examination which included indirect oph-

thalmoscopy, slit-lamp biomicroscopy with contact lens, FA, and spectral domain OCT (CIRRUS HD-OCT; Carl Zeiss Meditec, Jena, Germany). All patients were treated with an intravitreal injection of 0.5 mg ranibizumab (Lucentis[®]; Genentech, South San Francisco, CA, USA) or 2 mg aflibercept (Eylea[®]; Regeneron Pharmaceuticals, Inc., Tarrytown, NY, USA; Bayer AG, Berlin, Germany). Pro re nata injections were performed when macular edema or serous retinal detachment was evident at the fovea on OCT sections. The best-corrected visual acuity (BCVA) was determined using the Landolt C chart and intraocular pressure measured at every visit.

Optical Coherence Tomography Angiography An OCTA scan of the 12×12 -mm regions was obtained. All scans were comprised of 500 A-scans per B-scan, repeated twice at each of the 500 B-scan positions. En face images of the retinal vessels were made from the total retina, based on automated layer segmentation performed by software installed in the OCTA device. Manual segmentation was performed to assess the total retina, if needed. We only selected images with a signal strength of seven or higher.

En Face OCT

SS-OCT had a scanning speed of 100,000 scans per second. The central wavelength of the probe beam was 1,050 nm, and the axial resolution of this system was $6.3 \mu\text{m}$ in tissue. The scans were obtained using an automated averaging system which was preliminarily set such that the slices were automatically averaged. We only selected images with a signal strength of seven or higher. The software can define distinct layers of the retina, such as the inner limiting membrane and retinal pigment epithelium. We extracted depth-integrated en face slab images using the built-in analysis software by selecting the layer between the automatically determined inner limiting membrane and retinal pigment epithelium. The en face image integrates the reflectivity of only the A-scan signal within the defined layer.

Definition of en Face OCT or OCTA Findings

Using depth-integrated images on en face OCT, we found lesions that contained multiple concave areas of low reflectivity within areas of high reflectivity, distributed in a reticular pattern, which was thought to be a cystic lesion due to retinal edema. We defined this cystic lesion, referred to as “honeycomb sign” in our previous study [9], as “a cluster of relatively low-signal, oval or polygonal lesions, completely surrounded by a clear septum.” To define the affected lesion of BRVO, we first identified an arteriovenous crossing, which corresponded to the vein occlusion based on fundus photographs, OCTA images, and FA. We then defined the area of the affected lesion in 12×12 -mm OCTA images, which were present upstream of this occlusion site.

Image Analysis

Vascular density (VD), vascular length (VL), vascular lacunarity, and fractal dimension (FD) were measured on 12×12 -mm scan images (Fig. 1a). In this study, two of the authors (S.A. and S.S.) defined the area of cystic lesion in en face OCT in a masked fashion, then subsequently cropped the corresponding vascular images, and calculated four vascular parameters. First, a retinal cystic area, namely, the honeycomb area in the en face retinal OCT slab image (Fig. 1b), was cropped from a $1,024 \times 1,024$ -pixel original image using the polygonal tool in Adobe Photoshop CC software (Adobe Systems, San Jose, CA, USA). Second, the same lesion

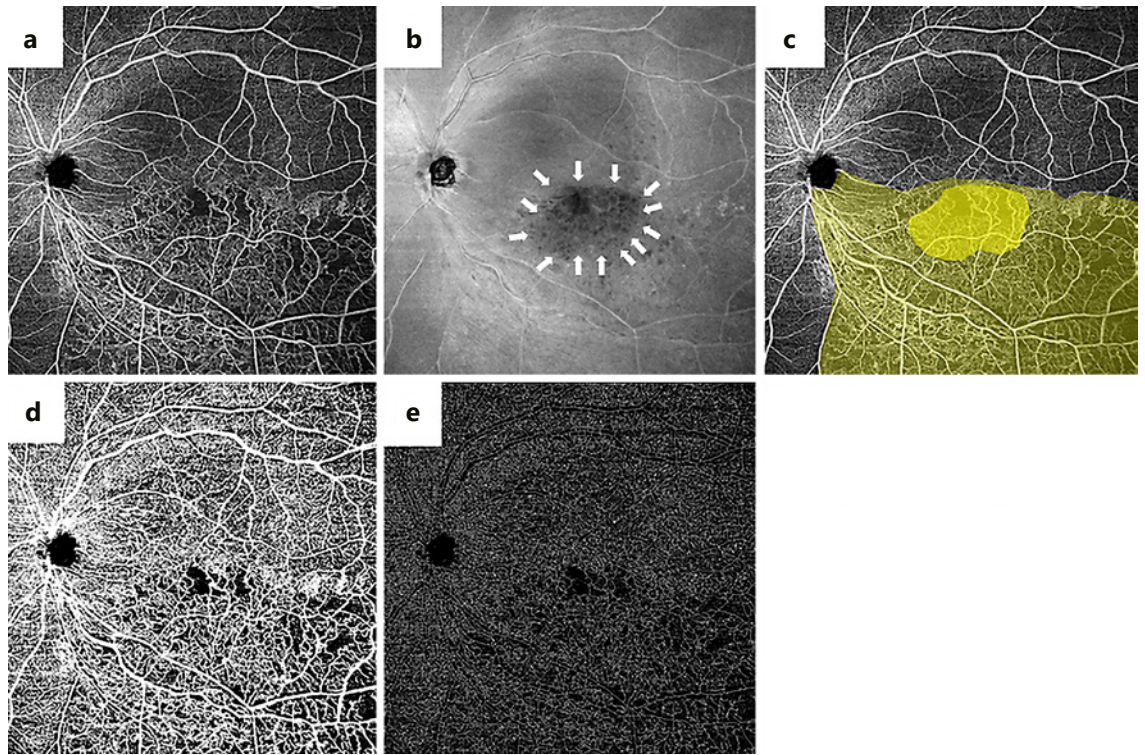


Fig. 1. Representative images of wide-field OCTA (a) and en face OCT (b). Arrows in (b) demonstrate the cystic lesion defined in this study. Lesion (c) affected by BRVO defined in (a) is highlighted by light yellow, and the area corresponding to the cystic lesion in (b) is highlighted by dark yellow. Contrast-enhanced binarized images for VD (d) and skeletonized (e) images for VL of the eyes with BRVO.

in the en face OCTA image of the cropped area was also cropped (Fig. 1c). The images of the corresponding honeycomb areas in the OCTA image were then binarized using a modified version of the previously reported procedure [5, 11] (Fig. 1d). The areas of these cystic lesions and other affected lesions were calculated using ImageJ software (Wayne Rasband, NIH). The images were converted to 8 bits, and a value of 255 (complete white) was assigned to all pixels with a positive gray level and a value of 0 (complete black) to the other pixels, using the contrast auto local threshold method (radius: 75 pixels; parameter 1: default; parameter 2: default) [12]. VD was defined as the ratio of the area occupied by the vessels and the total area. Vascular lacunarity, which characterizes oddities identified when vessel organization is disrupted significantly, may be useful for characterizing and quantitatively analyzing vascular networks in drug-treated specimens [13]. Vascular lacunarity and FD were calculated on the binarized image (Fig. 1e) using the Fraclac plugin for ImageJ software (Wayne Rasband, NIH); the box counting method was used. The vascular lacunarity and FD range from 0 to 2, and images with a more complex vessel branching pattern would have a higher FD.

Statistical Analysis

The BCVA values were converted to the logarithm of the minimal angle of resolution (logMAR) for all analyses. The data were analyzed using GraphPad Prism (GraphPad Software Inc., La Jolla, CA, USA). To compare various vascular parameters, the paired *t*

test or unpaired Student *t* test was performed as appropriate. In addition, linear regression analysis was performed to examine the association between VD and various factors. Statistical significance was set at $p < 0.05$.

Results

In this study, 66 patients who underwent wide-field SS-OCTA were enrolled. Among them, the eyes of 4 patients underwent pars plana vitrectomy and eight had co-existing diseases that could affect the outcomes of this study. Due to image quality issues in en face OCT slab images and en face OCTA images, we excluded 11 eyes and finally analyzed 43 eyes of 17 men and 26 women. Table 1 shows the patients' demographic data and ocular characteristics. The mean age of the patients at the time of examination was 68.9 ± 11.2 years (range: 45–90 years). The mean BCVA at baseline was 0.24 ± 0.29 (range: -0.18 to 1.00) in logMAR equivalent. The mean number of anti-VEGF drug injections administered before the examination was 4.1 ± 3.8 (range: 1–16). The mean duration

Table 1. Patient characteristics

Parameter	Data
Mean, age \pm SD, years	68.9 \pm 11.2 years (range: 45–90 years)
Gender (male/female; <i>n</i>)	(17/26)
BCVA (logMAR) at initial visit (mean \pm SD)	0.24 \pm 0.29 (range: –0.18 to 1.00)
BCVA (logMAR) on examination (mean \pm SD)	0.15 \pm 0.30 (range: –0.2 to 1.0)
Duration	15.3 \pm 13.7 months (range: 3–58 months)
No. of anti-VEGF injections (mean \pm SD)	8.8 \pm 9.6
Distribution of retinal cystic lesion, <i>n</i> (%)	
No cystic lesion	13 eyes (30.2)
Cystic lesion in the macula within two-disk diameter area	15 eyes (34.9)
Cystic lesion outside the macula but within the vascular arcade	10 eyes (23.3)
Cystic lesion outside the vascular arcade	5 eyes (11.6)
Mean area of cystic lesion	8.5 \pm 10.1 mm ²
Mean area of affected lesion	38.7 \pm 19.8 mm ²

BCVA, best-corrected visual acuity; VEGF, vascular endothelial growth factor.

Table 2. Factors associated with VD in the cystic lesions in the involved eyes within vascular arcade

Factors	Coefficient	<i>p</i> value
BCVA (logMAR) at initial visit	–0.263	0.202
BCVA (logMAR) on examination	–0.433	0.0492
Duration	–0.111	0.567
Anti-VEGF injections, <i>n</i>	0.135	0.505

BCVA, best-corrected visual acuity; VEGF, vascular endothelial growth factor.

from the baseline visit to the time when OCTAs were performed was 15.3 \pm 13.7 months (range: 3–58 months). The mean BCVA when OCTAs were performed was 0.15 \pm 0.30 (range: –0.2 to 1.0) in logMAR equivalent.

The distribution of retinal cystic lesions detected by en face OCT was as follows: no cystic lesion in 13 eyes (30.2%), cystic lesion in the macula within a two-disk diameter area in 15 eyes (34.9%), cystic lesion outside the macula but within the vascular arcade in 10 eyes (23.3%), and cystic lesion outside the vascular arcade in 5 eyes (11.6%). The mean area of the cystic lesions was 8.5 \pm 10.1 mm² and that of the affected lesions was 38.7 \pm 19.8 mm². Next, we calculated and compared various vascular parameters present in the cystic lesions with those in the other BRVO-affected areas. We compared each vascular parameter of the retinal cystic area with the noncystic area in all 30 eyes associated with a retinal cystic lesion (“same eyes” in Fig. 2). In addition, as this study included

13 eyes of no cystic lesion, we compared vascular parameters of the retinal cystic area in all 30 eyes associated with retinal cystic lesion with nonretinal cystic area in all 43 eyes (“total series” in Fig. 2). The mean VD in the cystic lesions was 25.6% \pm 16.9% (2.4–72.4%). VD in the other affected areas of the same eyes was 36.5% \pm 13.5% (range: 17.5–66.0%, *p* = 0.0010) and in total series was 33.5% \pm 14.1% (range: 17.5–78.7%, *p* = 0.0281) (Fig. 2a). The mean VL in the cystic lesions was 6.41 \pm 3.80 mm (range: 0.21–14.5 mm). VL in the other affected areas of the same eyes was 9.29 \pm 2.55 mm (range: 5.31–14.2 mm, *p* = 0.0001) and in total series was 8.73 \pm 2.75 mm (range: 4.64–16.7 mm, *p* = 0.0050) (Fig. 2b). The mean vascular lacunarity in the cystic lesions was 0.69 \pm 0.21 (range: 0.32–1.21). Vascular lacunarity in the other affected areas of the same eyes was 0.67 \pm 0.18 (range: 0.41–1.26, *p* = 0.635) and in total series was 0.66 \pm 0.21 (range: 0.41–1.36, *p* = 0.566) (Fig. 2c). The mean FD in the cystic lesions was 1.41 \pm 0.38 (range: 0.55–1.76). FD in the other affected areas of the same eyes was 1.71 \pm 0.08 (range: 1.83–1.51, *p* = 0.0003) and in total series was 1.72 \pm 0.07 (range: 1.51–1.83, *p* < 0.0001) (Fig. 2d). Finally, VD in cystic lesions within the vascular arcade correlated with BCVA on OCTA (*r* = –0.433, *p* = 0.0492, Table 2).

Discussion

In the current study, we quantitatively evaluated the morphology of the microvasculature in the retinal cystic lesions associated with BRVO using wide-field SS-OC-

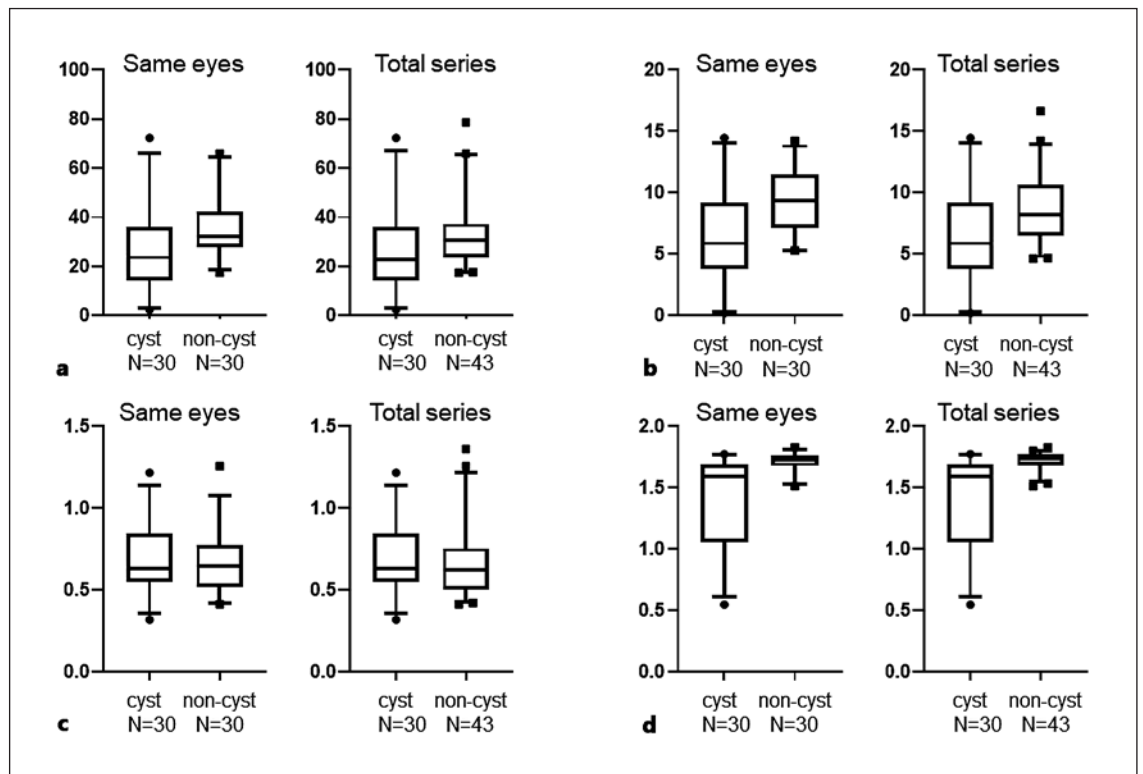


Fig. 2. Box plots of vascular parameters in the cystic lesion compared with that in the other affected areas of the same eyes or in all eyes. **a** VD in the cystic lesion compared with that in the other affected areas of the same eyes (left, $p = 0.001$) or in total series (right, $p = 0.0281$). **b** VL in the cystic lesion compared with that in the other affected areas of the same eyes (left, $p = 0.0001$) or in total series (right, $p = 0.005$). **c** Vascular lacunarity in the cystic lesion compared with that in the other affected areas of the same eyes (left, $p = 0.6354$) or in total series (right, $p = 0.5659$). **d** FD in the cystic lesion compared with that in the other affected areas of the same eyes (left, $p = 0.0003$) or in total series (right, $p < 0.0001$).

TA. En face OCTA images combined with en face OCT images derived from depth-integrated reflectivity of the retina showed that VD, VL, and FD were decreased in cystic retinal edema. These findings may help in understanding the pathophysiology of retinal edema associated with BRVO.

In a previous study, researchers reported methods for visualizing the inner retina of the nonperfused area in eyes with BRVO, namely, by summing the signals of the neural retina from the en face SS-OCT images; cystic changes were highly corresponded to the nonperfused area [9]. On B-scan images of the area with cystic changes, large retinal cysts were detected throughout all retinal layers. However, after the administration of anti-VEGF drugs, the honeycomb signs decreased, retinal edema resolved, and the neural retina thinned. One of the limitations of our previous study was that we independently analyzed the FA image and en face SS-OCT image. In

contrast, the current study applied wide-field OCTA, which simultaneously acquired en face OCTA and OCT images. We found that the microvasculature in the cystic lesion showed decreased vascular parameters such as VD, VL, and FD.

A previous study demonstrated that the macular thickness was affected by the extent of macular perfusion; the partially perfused capillary area, not the area of complete capillary loss, affected macular edema associated with BRVO [10]. The partially perfused areas, which represent dilated, tortuous vessels, were often present within the hypofluorescent areas in FA images. Our hypothesis on these findings was that dilated capillaries accommodated various pathological changes, including hypoxia, increased influx due to occlusion of other capillaries, and loss of pericytes. This hypothesis is supported by a previous study which reported that an increased luminal pressure increases the transduction of blood and interstitial

fluid pressure [9, 14], as well as recent reports that described the findings of macular edema with perfusion status utilizing OCTA to treat BRVO [10, 15].

Comparative analysis of OCTA parameters in cystic lesions showed that VD, VL, and FD were significant factors. Hirano et al. [16] reported that VD, VL, and FD progressively decreased with worsening DR in segmented and nonsegmented layers of 3 × 3-mm, 6 × 6-mm, and 12 × 12-mm SS-OCTA scan sizes [16]. We demonstrated the efficacy of wide-field SS-OCTA in eyes with BRVO by using parameters such as VD and VL to detect retinal non-perfusion [4, 12]. VL was first invented as a method to quantify magnetic resonance angiography [17] and has recently been applied to OCTA [18]. VL is reportedly adequate for detecting smaller vessels [4]. Hirano et al. [16] demonstrated that the area under the curve of VD decreased with the increase in scan size in eyes with DR; however, the area under the curve of VL did not decrease as much as that of VD in the progression of DR. This may be due to the larger blood vessels being involved in a larger image. The pathology of BRVO involves the microvasculature; hence, the effects of smaller vessels may be masked if the image includes larger blood vessels.

A limitation of the current study was the inclusion of patients with relatively chronic BRVO because OCTA image acquisition is difficult before retinal hemorrhages resolve. Another limitation was the retrospective and cross-sectional nature of the study; therefore, the timing of OCTA examination in the patients was not controlled. In addition, we did not perform any inter-observer or intra-observer correlation coefficient in the current study. Furthermore, anti-VEGF therapy during the follow-up period could affect the development of retinal cysts. However, we excluded eyes that received an injection 3 months before the examination.

In conclusion, wide-field SS-OCTA analysis, combined with en face OCT images, provided information on how the microvasculature changes simultaneously with the development of retinal cystic lesions, that is, decreased VD, shorter VL, and lower FD in the area of retinal cysts.

The current findings contribute to the understanding of the pathophysiology of BRVO. While further studies are warranted to confirm these findings, we believe that a more cautious, individualized approach to BRVO care, with close monitoring using wide-field SS-OCTA, should be considered.

Statement of Ethics

This research was conducted ethically in accordance with the World Medical Association Declaration of Helsinki. The institutional review board of Osaka University Hospital approved the study protocol (approval number: 09260), and informed consent was obtained from the patients after an explanation of the nature and possible consequences of the study.

Conflict of Interest Statement

The authors declare no competing interests.

Funding Sources

There is no funding resource.

Author Contributions

Conception and design: Satoko Araki and Susumu Sakimoto. Analysis and interpretation: Satoko Araki, Susumu Sakimoto, and Daiki Shiozaki. Data collection: Satoko Araki, Susumu Sakimoto, Daiki Shiozaki, Chihiro Ueda, Chikako Hara, Yoko Fukushima, and Kaori Sayanagi. Supervision: Hirokazu Sakaguchi and Kohji Nishida. All authors reviewed the manuscript.

Data Availability Statement

All data generated or analyzed during this study are included in this article. Further inquiries can be directed to the corresponding author.

References

- 1 Rogers SL, McIntosh RL, Lim L, Mitchell P, Cheung N, Kowalski JW, et al. Natural history of branch retinal vein occlusion: an evidence-based systematic review. *Ophthalmology*. 2010 Jun;117(6):1094–101.e5.
- 2 Campochiaro PA, Heier JS, Feiner L, Gray S, Saroj N, Rundle AC, et al. Ranibizumab for macular edema following branch retinal vein occlusion: six-month primary end point results of a phase III study. *Ophthalmology*. 2010 Jun;117(6):1102–12.e1.
- 3 Campochiaro PA, Bhisitkul RB, Shapiro H, Rubio RG. Vascular endothelial growth factor promotes progressive retinal nonperfusion in patients with retinal vein occlusion. *Ophthalmology*. 2013 Apr;120(4):795–802.
- 4 Shiraki A, Sakimoto S, Tsuboi K, Wakabayashi T, Hara C, Fukushima Y, et al. Evaluation of retinal nonperfusion in branch retinal vein occlusion using wide-field optical coherence tomography angiography. *Acta Ophthalmol*. 2019 Sep;97(6):e913–8.

- 5 Shiozaki D, Sakimoto S, Shiraki A, Wakabayashi T, Fukushima Y, Oie Y, et al. Observation of treated iris neovascularization by swept-source-based en-face anterior-segment optical coherence tomography angiography. *Sci Rep*. 2019 Jul;9(1):10262.
- 6 Nagiel A, Sadda SR, Sarraf DA. A promising future for optical coherence tomography angiography. *JAMA Ophthalmol*. 2015 Jun;133(60):629–30.
- 7 Jia Y, Bailey ST, Hwang TS, McClintic SM, Gao SS, Pennesi ME, et al. Quantitative optical coherence tomography angiography of vascular abnormalities in the living human eye. *Proc Natl Acad Sci U S A*. 2015 May;112(18):E2395–402.
- 8 Samara WA, Shahlaee A, Sridhar J, Khan MA, Ho AC, Hsu J. Quantitative optical coherence tomography angiography features and visual function in eyes with branch retinal vein occlusion. *Am J Ophthalmol*. 2016 Jun;166:76–83.
- 9 Sakimoto S, Gomi F, Sakaguchi H, Akiba M, Kamei M, Nishida K. Analysis of retinal non-perfusion using depth-integrated optical coherence tomography images in eyes with branch retinal vein occlusion. *Invest Ophthalmol Vis Sci*. 2015 Jan;56(1):640–6.
- 10 Sakimoto S, Kamei M, Suzuki M, Yano S, Matsumura N, Sakaguchi H, et al. Relationship between grades of macular perfusion and foveal thickness in branch retinal vein occlusion. *Clin Ophthalmol*. 2013;7:39–45.
- 11 Sophie R, Hafiz G, Scott AW, Zimmer-Galler I, Nguyen QD, Ying H, et al. Long-term outcomes in ranibizumab-treated patients with retinal vein occlusion: the role of progression of retinal nonperfusion. *Am J Ophthalmol*. 2013 Oct;156(4):693–705.
- 12 Tsuboi K, Ishida Y, Kamei M. Gap in capillary perfusion on optical coherence tomography angiography associated with persistent macular edema in branch retinal vein occlusion. *Invest Ophthalmol Vis Sci*. 2017 Apr;58(4):2038–43.
- 13 Zudaire E, Gambardella L, Kurcz C, Vermeren S. A computational tool for quantitative analysis of vascular networks. *PLoS One*. 2011;6(11):e27385.
- 14 Campo Chiaro PA, Hafiz G, Shah SM, Nguyen QD, Ying H, Do DV, et al. Ranibizumab for macular edema due to retinal vein occlusions: implication of VEGF as a critical stimulator. *Mol Ther*. 2008 Apr;16(4):791–9.
- 15 Hasegawa T, Takahashi Y, Maruko I, Kogure A, Iida T. Macular vessel reduction as predictor for recurrence of macular oedema requiring repeat intravitreal ranibizumab injection in eyes with branch retinal vein occlusion. *Br J Ophthalmol*. 2019 Oct;103(10):1367–72.
- 16 Hirano T, Kitahara J, Toriyama Y, Kasamatsu H, Murata T, Sadda S. Quantifying vascular density and morphology using different swept-source optical coherence tomography angiographic scan patterns in diabetic retinopathy. *Br J Ophthalmol*. 2019 Feb;103(2):216–21.
- 17 Yim PJ, Choyke PL, Summers RM. Gray-scale skeletonization of small vessels in magnetic resonance angiography. *IEEE Trans Med Imaging*. 2000 Jun;19(6):568–76.
- 18 Agemy SA, Sripsema NK, Shah CM, Chui T, Garcia PM, Lee JG, et al. Retinal vascular perfusion density mapping using optical coherence tomography angiography in normals and diabetic retinopathy patients. *Retina*. 2015 Nov;35(11):2353–63.